The hybrid pressurized air receiver (HPAR) in the SUNDISC cycle

Lukas Heller, Jaap Hoffmann, and Paul Gauché

Citation: AIP Conference Proceedings **1734**, 030019 (2016); doi: 10.1063/1.4949071
View online: http://dx.doi.org/10.1063/1.4949071
View Table of Contents: http://scitation.aip.org/content/aip/proceeding/aipcp/1734?ver=pdfcov
Published by the AIP Publishing

The Hybrid Pressurized Air Receiver (HPAR) in the SUNDISC Cycle

Lukas Heller[1,a)], Jaap Hoffmann[1] and Paul Gauché[1]

[1]*Solar Thermal Energy Research Group, Stellenbosch University, Private Bag X1, Matieland 7602, Stellenbosch, South Africa*

[a)]Corresponding author: Lukas_Heller@gmx.de

Abstract. Tubular metallic pressurized air solar receivers face challenges in terms of temperature distribution on the absorber tubes and the limited sustainable solar influx. The HPAR concept aims at mitigating these problems through a macro-volumetric design and a secondary non-pressurized air flow around the absorber elements. Here, a 360° manifestation of this concept for implementation in the dual-pressure SUNDISC cycle is presented. Computationally inexpensive models for the numerous heat flows were developed for use in parametric studies of a receiver's geometric layout. Initial findings are presented on the optical penetration of concentrated solar radiation into the absorber structure, blocking of thermal radiation from hot surfaces and the influence of the flow path through the heated tubes. In the basic design the heat transfer to the non-pressurized air stream is found to be insufficient and possible measures for its improvement are given. Their effect will be examined in more detailed models of external convection and thermal radiation to be able to provide performance estimates of the system.

INTRODUCTION

Pressurized air solar receivers enable the use of highly efficient combined cycles in central receiver concentrating solar power (CSP) plants. Previously developed technologies can be grouped into those utilizing volumetric ceramic absorbers with pressurized quartz glass windows and those using tubular metallic absorbers. The former can reach air outlet temperatures above 1200 °C [1] and thermal efficiencies above 80 % [2]. However, their quartz glass windows pose challenges in terms of durability [3] and the optical efficiency is generally low due to the need for secondary concentrators and polar solar fields.

The high cost of high-temperature receivers led to the development of more cost-effective and potentially robust designs for preheating pressurized air [4]. These preheaters commonly feature metallic absorber tubes inside a cavity, which limits their outlet temperature to approximately 800 °C and negatively influences the solar field efficiency. Problems with tubular air receivers mainly arise due to the disadvantageous heat transfer properties of air and the non-uniform impinging flux onto the tubes, resulting in high temperature gradients between the irradiated front of the tubes and their back as well as between the tube and the air flow. This temperature distribution leads to high thermal stresses of the material and elevated thermal losses due to the high temperatures of the ambient-facing surfaces [5].

In this study a receiver concept is presented that addresses some of the most problematic issues with previously investigated metallic tubular air preheaters, namely, the temperature distribution, the optical constrains on the solar field and the limited impinging flux on the absorber. The concept is furthermore adapted to a thermodynamic cycle that takes full advantage of its characteristics and a possible system configuration is shown. Finally, initial modeling of the heat transfer mechanisms and findings on this receiver manifestation are presented.

THE HPAR CONCEPT

The Hybrid Pressurized Air Receiver (HPAR) concept, first introduced by Kretzschmar and Gauché [6], describes an air receiver in which bundles of tubes are the absorbers of solar radiation (see Fig. 1). As in other proposed and developed pressurized air receivers, the air stream downstream the compressor is heated as it passes through the inside

SolarPACES 2015
AIP Conf. Proc. 1734, 030019-1–030019-8; doi: 10.1063/1.4949071
Published by AIP Publishing. 978-0-7354-1386-3/$30.00

of these tubes before it enters the combustion chamber of the gas turbine or a high-temperature high-pressure receiver system.

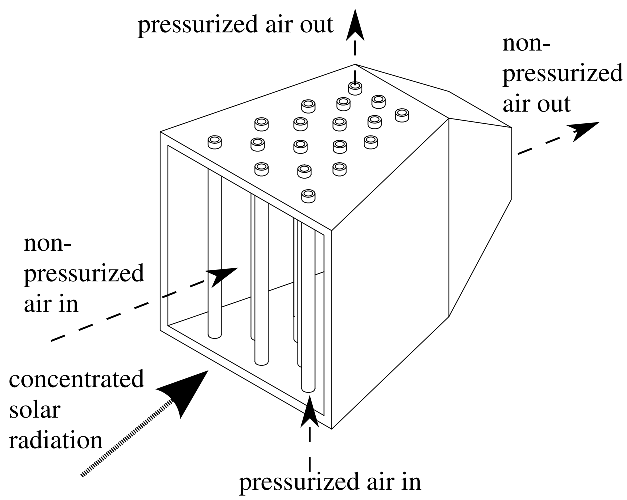

FIGURE 1. Sketch of the HPAR concept (adapted from Heller and Gauché [7])

The staggered arrangement of the tubes is intended to create a 'macro-volumetric' absorber with a small surface area exposed to ambient but a large heat transfer area to the heat transfer fluids. Thermal radiation and reflected concentrated solar irradiation from the tubes are partially absorbed by other tubes instead of being lost to the surroundings. Ideally, the highest absorber temperature in such a receiver is apparent at tubes inside the cavity as opposed to external receivers where the outermost surfaces have the highest temperature. Heating up of the air would advantageously start at the highly irradiated and exposed front before flowing through a serpentine path towards the 'shielded' back. The combination of the temperature increase towards the inside of the receiver and the increased convective heat transfer surface compared to the receiver aperture area is commonly referred to as the 'volumetric effect' [8].

The second defining feature of the HPAR is a non-pressurized air flow around the tubes of the bundle (see Fig. 1). This forced flow cools the tube surfaces by means of convection and evens out the circumferential temperature gradients on the tubes, therefore decreasing thermal stresses. The coldest air is in contact with the most exposed surfaces of the bundle, enabling a strong cooling effect (depending on flow conditions) and further minimizing losses due to thermal radiation from the exposed frontal rows.

In a single-pressure receiver system, thermal energy transferred to ambient air via natural convection would be discarded. This convection loss can account for approximately 10 % of the incoming concentrated radiation in a cavity receiver [9]. In the HPAR concept, the thermal energy is not lost but used as a source of lower-temperature thermal energy to the cycle. However, as the convection heat transfer to the non-pressurized air stream is enforced, the maximum energy input to the pressurized air stream decreases. The value of the receiver concept, therefore, largely depends on a beneficial introduction of this lower-grade heat into the cycle. A suitable cycle along with the implementation of a manifestation of the HPAR concept is presented in the following section.

ADAPTATION OF THE HPAR CONCEPT TO THE SUNDISC CYCLE

It has previously been shown that combined (Brayton and Rankine) cycle CSP plants with a passive thermal energy storage system downstream the gas turbine have inherent limitations in terms of achievable solar fraction and capacity factor [7]. To overcome these shortcomings, a combined cycle featuring a dual-pressure air receiver system was proposed (SUNDISC cycle).

Figure 2 depicts a variation of the SUNDISC cycle with a hybrid receiver system (HRS) as the preheater of compressed air and the heater of a non-pressurized air flow. It also includes a high-temperature high-pressure receiver system (HT-HPRS) to further increase the (optional) combustion chamber inlet temperature. While separated receiver systems for the pressurized air pre-heating and unpressurized air heating are possible, a hybrid receiver solution with a manifestation of the HPAR concept is thought to be energetically and economically advantageous. The reasons being

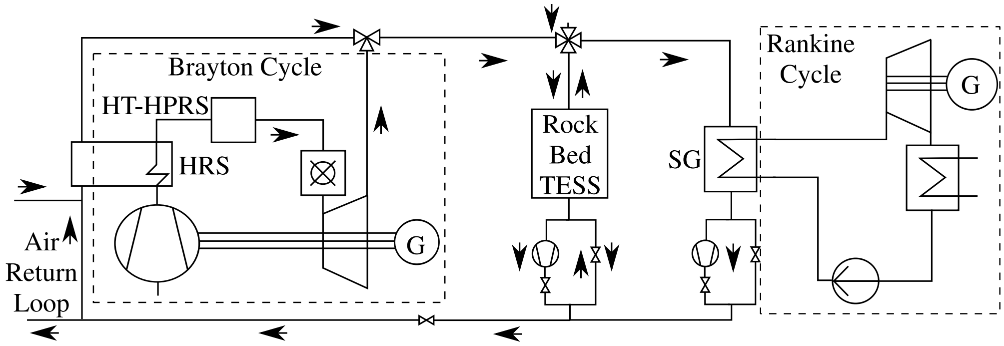

FIGURE 2. Schematic of the SUNDISC cycle with cascaded hybrid receiver system

an increased receiver rating due to the dual-cooling of the absorber elements as well as the previously mentioned augmented volumetric effect. The HT-HPRS is expected to feature receivers of the volumetric type with pressurized quartz glass windows that increase the air temperature to above 1000 °C while the 'low-temperature' HRS could feature a metallic tubular absorber and preheat the pressurized air to approximately 800 °C. The non-pressurized air stream should ideally be heated to the same temperature as the gas turbine outlet (approximately 540 °C) so that both streams can simultaneously charge the thermal energy storage system (TESS) or power the steam generator (SG) without further loss of exergy. A return loop of the exhaust gas from the TESS and SG to the non-pressurized inlet stream of the HRS is a likely option if found feasible and viable.

A rendering of a possible manifestation of the two receiver systems and the connecting piping can be seen in Fig. 3. The HT-HPRS could be located on the northern side of the tower (for a northern hemisphere plant) to benefit from the highest annual solar field efficiency, lowered spillage losses and shorter piping at the highest temperature while the 360° HPAR receiver allows for the utilization of a surrounding field.

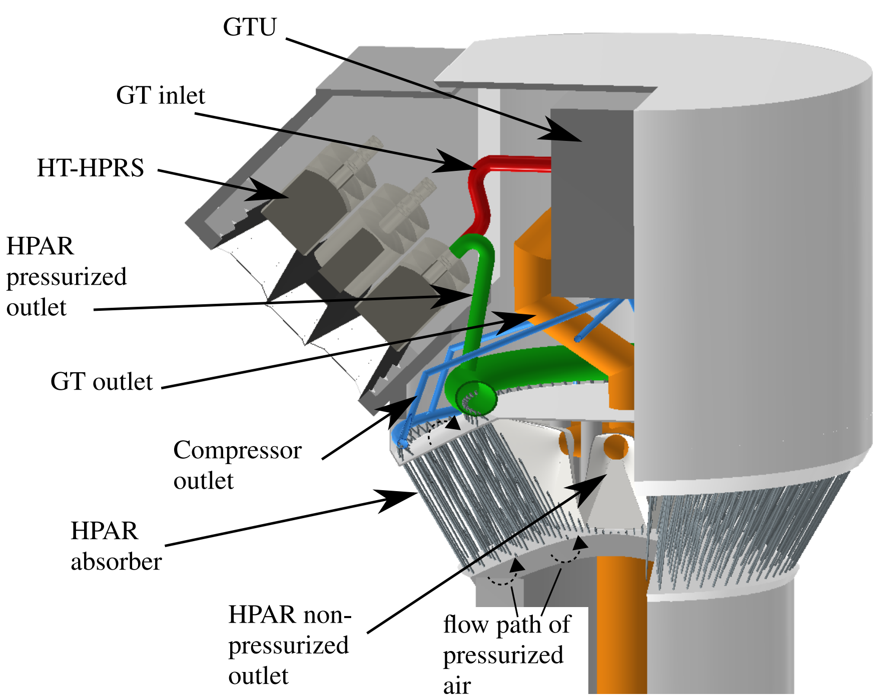

FIGURE 3. Rendering of a manifestation of a cascaded hybrid receiver system (dimensions not to scale)

TABLE 1. Boundary conditions of the investigated receiver system

Parameter	Value	Reference
GTU rating	5.25 MW_e	[12]
Pressurized air mass flow	20.5 kg/s	[12]
Operating pressure	14.7 bar	[12]
Compressor outlet temperature	400 °C	[12]
GT outlet/desired HPAR non-pressurized air outlet temperature	540 °C	[12]
HPAR pressurized air outlet temperature	800 °C	[11]
Absorber tube maximum temperature	900 °C	[13]
Absorber tube inner/outer diameter	25 mm/30 mm	[11]
Maximum pressure drop	100 mbar	see paragraph

INITIAL MODELING AND FINDINGS

The overall performance of an HPAR receiver is dictated by the effectiveness of absorbing incoming concentrated solar radiation and the ability to transfer the absorbed thermal energy to the air streams. For an overall energy balance of the receiver, detailed heat transfer modeling is therefore necessary for the following energy flows:

- Absorption and reflection of incoming solar radiation,
- internal forced convection to the pressurized air stream,
- radiation heat transfer between tubes, walls and ambient as well as
- external forced/mixed convection to the non-pressurized air stream.

In the following sections, models of different levels of detail are presented for these mechanisms. These models are primarily intended to provide insights to the interaction of the energy flows and help identify sensible geometrical parameters for later, more in-depth simulations. Boundary conditions and performance indicators are derived from the chosen implementation of the HPAR in a SUNDISC cycle plant with a cascaded hybrid receiver system.

Boundary Conditions

The chosen boundary conditions are derived from previous analyses of a SUNDISC cycle plant [10] and similar receiver developments. A selection of the chosen values can be found in Table 1. The maximum allowable pressure drop was deduced from an allowable system pressure drop between compressor outlet and turbine inlet of 250 mbar [11] and estimates on the pressure drops of the HT-HPRS, the connecting piping and fittings.

Optical Penetration

One of the aims of the HPAR concept's staggered tube bundle design is to imitate the effect of a cavity by absorbing incoming radiation on surfaces that are at least partially shielded from the environment. The deeper the radiation penetrates, the more thermal energy can be transferred from surfaces that have reduced view factors to the environment and the more even the thermal input to the tubes, the better the utilization of all absorber tubes.

As the geometric tube bundle layout that generates the deepest penetration or most uniform flux distribution on the absorbers is not obviously identifiable, a ray-tracing study with varying geometrical parameters has been conducted in SolTrace V. 2012.7.9 [14]. In order to simulate realistic influx on absorber tubes, the heliostat field is modeled based on an existing layout, namely the field of eSolar's Sierra SunTower for which limited validation data is available [15]. The absorber tubes are modeled with the optical properties of Pyromark 2500 paint [16] and the walls are given an absorption coefficient of 0.3 in the solar spectrum [17]. Assumptions for the geometrical layout that were not varied include that

- the receiver is tilted by a non-optimized angle of 45°,
- the number of tubes per row is identical and
- the distance between rows is identical.

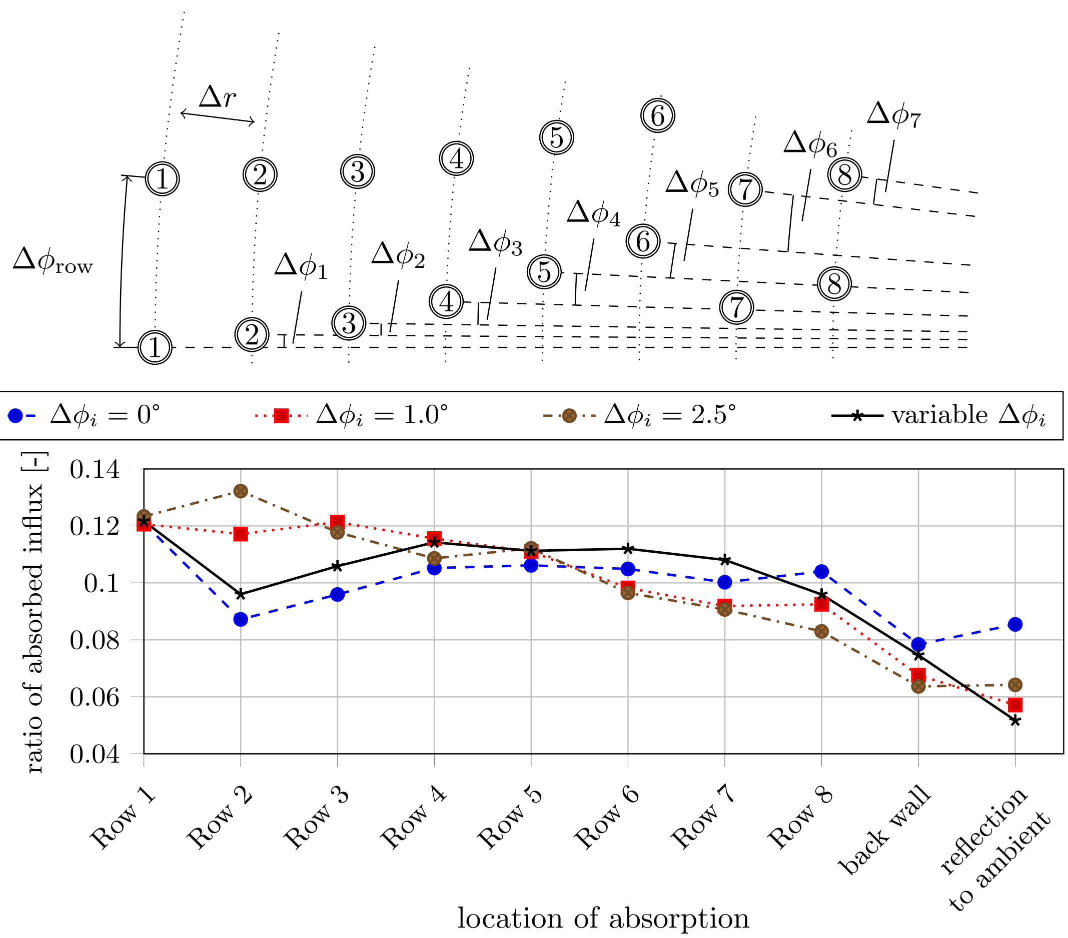

FIGURE 4. Distribution of absorbed incoming flux in the absorber tube rows for constant and variable angular offsets, $\Delta\phi_i$, between tube rows. The counter-intuitive behavior of increasing absorption between Row 1 and Row 2 for $\Delta\phi_i = 2.5°$ is due to the increasing tube density towards the center of the receiver. Additionally, in this particular layout, shading is especially low because of the large angular offset.

In successive design point simulations the angle between the tubes in a row, $\Delta\phi_{\text{row}}$, and the tangential offset of each tube row to the next, $\Delta\phi_i$, was varied and the ratio of absorbed radiation in each row over the total incoming radiation calculated. While the absorbed radiation in the front row is almost entirely defined by the angle between the tubes, the distance from the center of the receiver and the tube diameter, the absorption in further rows is strongly influenced by the tangential offset. The distribution of the absorbed flux per row for layouts with identical offsets between all rows is depicted in Fig. 4. Additionally, the distribution for one layout with varying offsets, which result in a relatively even flux profile, is shown. The authors acknowledge that this distribution is bound to change over the cause of a day and year as blocking, shading and cosine efficiencies change. However, it is shown that considerable penetration into the tube bundle is feasible and that the angular offset between tube rows has a major influence on the absorption distribution.

Thermal Radiation

At the elevated temperatures the HPAR is designed for, thermal radiation will have a significant impact on the receiver's energy balance. For the current study, a simplified radiation model of the receiver was developed to allow for computationally inexpensive simulations for parametric studies. Simplifications include that

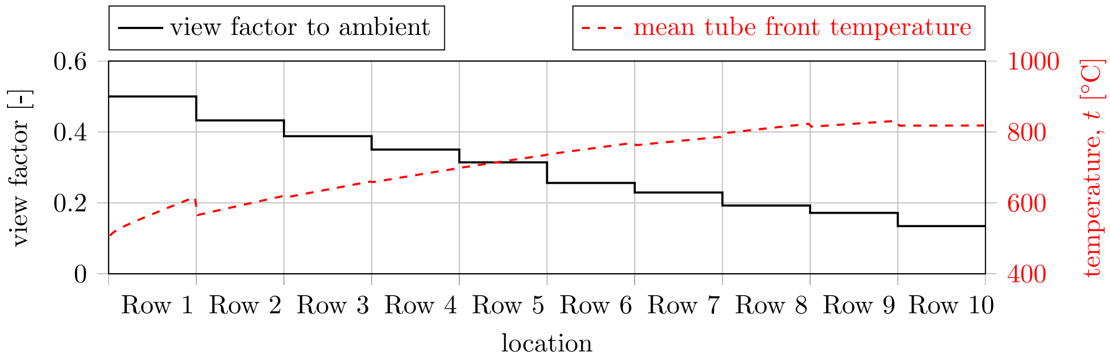

FIGURE 5. View factors to ambient and mean tube front temperatures in a 8-row setup with serial flow path

- the tubes have a binary temperature profile (back/front) and
- all tubes are infinitely long and parallel (no tilt).

Figure 5 depicts each row's respective view factor to ambient in one chosen layout and one possible temperature layout (derived from the model with a serial flow path in the following section). The desired inverse distribution of surface temperature and view factor to ambient is pronounced for this layout.

Internal Forced Convection

Convection to fluid flows in circular tubes is one of the most commonly investigated heat transfer problems, leading to numerous empirical correlations for it. In the developed model, Gnielinski's equation [18, Chapter G1] for the local Nusselt number was implemented to calculate the mean heat transfer for an axial flow segment, j,

$$Nu_j = \frac{\left(f_j/8\right) Re_j \, Pr_j}{1 + 12.7\,\sqrt{f_j/8}\,\left(Pr_j^{2/3} - 1\right)} \left[1 + 1/3\left(\frac{D_\mathrm{i}}{x}\right)^{2/3}\right]. \qquad (1)$$

Wherein Re and Pr are the Reynolds and Prandtl numbers, respectively, f is the Darcy-Weisbach friction factor, D_i is the inner tube diameter and x is the distance from the tube inlet. The local heat transfer in a circumferential segment is then derived from the heat flux distribution around the inner circumference of the tube according to a method developed by Reynolds [19] and Gärtner, Johannsen, and Ramm [20].

Due to the maximum allowable pressure drop, the flow velocity and flow path length (number of tubes in series) are limited. One possibility to increase the flow velocity — and therefore the heat transfer in the tubes and the receiver's thermal efficiency — is to split the flow into several paths of which each only runs through a fraction of the tubes. The different temperature profiles for one layout with a single serial flow path and one with two parallel paths are depicted in Fig. 6. The flow velocities were adapted so that both generate the identical pressure drop, however, the solar influx was adjusted to not exceed the allowable material temperatures. The optimum layout will eventually have to be identified taking into account the differing thermal losses of a receiver design.

External Forced Convection

The heat transfer from the tube surfaces to the non-pressurized air flow is calculated with correlations for tube bundles [18, Chapter G7]. These correlations are, however, intended for overall heat transfer of a tube bundle and not for deriving detailed temperature and heat transfer coefficient profiles around the individual tubes. The found results are to be seen as rough estimates for the potential of heating up this air stream. More elaborate simulations of the fluid domain in CFD are expected to provide more detailed results.

Simulations with the described model indicate external Nusselt number values several times lower than on the inner tube surface. This results in only a small cooling effect and insufficient outlet temperatures of the external air flow compared to the GT exhaust gas temperature even at low flow velocities (<1 m/s). Additionally to the low thermal input to the bottoming cycle, it is expected that wind effects will play a major role at these low velocities with further negative effects on operability and efficiency of the receiver system.

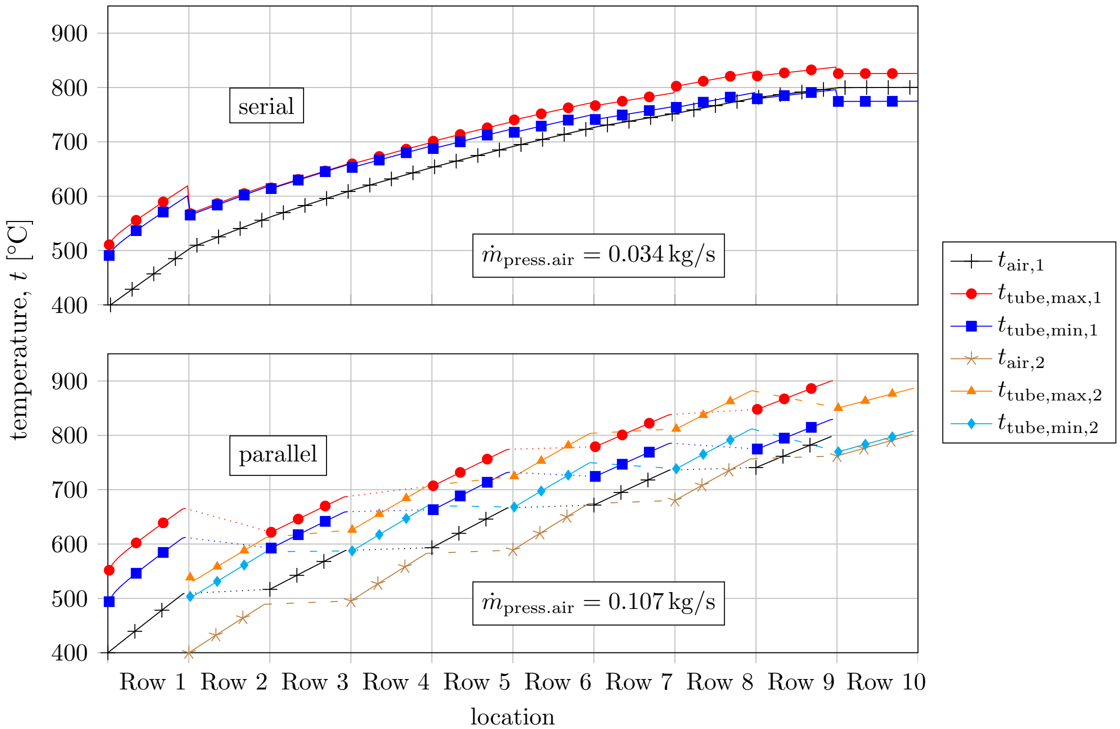

FIGURE 6. Temperatures of tubes and air flow for serial and parallel flow paths, respectively (the number in the variables' subscripts indicates the flow path)

To increase the heat transfer to the external air stream and shield the receiver from wind effects, a number of measures are conceivable, namely

- quartz glass inserts as wind shields,
- quartz glass inserts to redirect the external air flow,
- jet impingement of the air return flow on highly irradiated surfaces,
- external heat transfer enhancements (fins) on tubes and
- an open volumetric receiver system in the center of the HPAR receiver to increase the air outlet temperature (similar to the concept presented by Buck *et al.* [21]).

CONCLUSION AND OUTLOOK

A dual-pressure air solar receiver based on the HPAR concept is presented as well as a manifestation of it which has been adapted to the SUNDISC cycle. The manifestation has tubular metallic absorbers that are cooled from two air streams, a pressurized stream on the inside of the tubes and a non-pressurized stream around their outside surfaces.

Simplified heat transfer models were created for the dominant energy flows to identify favorable geometric layouts and flow paths for further development as well as problematic areas and properties. Firstly, the optical penetration was modeled in a ray-tracing model to quantify the penetration of incoming solar flux. It was found that the geometrical layout greatly influences the distribution of the heat flux on the absorber tube rows. Secondly, models for radiative and internal forced convective heat transfer were developed. They show the potential benefit of different flow paths, however, more elaborate interconnected models are needed to confirm these findings. Internal heat transfer enhancements are a further possibility to lower the tube temperatures at the cost of higher pressure drops.

The external convective heat transfer was modeled with high-level correlations for tube bundles which do not account for the detailed geometry of the receiver. Simulations with these models showed that the achievable external heat transfer with the basic investigated design is insufficient to reach the intended outlet temperature of the non-pressurized fluid. However, several potential enhancements are proposed to increase the outlet temperature and efficiency as well as the system's operating stability. To evaluate the effectiveness of the enhancements, the external flow will be examined in more detailed CFD models. With these same models thermal radiation between the tubes and to the environment will also be simulated with increased accuracy. Once all models are validated and merged, the design-point performance of an HPAR system within the SUNDISC cycle can be estimated and its off-design performance and operability can be studied.

ACKNOWLEDGEMENTS

The authors would like to thank the Solar Thermal Energy Research Group (STERG), the Centre for Sustainable and Renewable Energy Studies (CRSES) and the Department of Mechanical and Mechatronic Engineering at Stellenbosch University for funding of the project and enabling its presentation at SolarPACES 2015.

REFERENCES

[1] A. Kribus, P. Doron, R. Rubin, R. Reuven, E. Taragan, S. Duchan, and J. Karni, Journal of Solar Energy Engineering **123**, p. 10 (2001).

[2] R. Buck, "Modularer Druck-Receiver für solarunterstützte fossile Gasturbinen- und Kombikraftwerke (REFOS-2) Schlußbericht," Tech. Rep. April (DLR, Stuttgart, 2003).

[3] A. Hofmann, C. Schenk, and R. Uhlig, "Optical quartz glass windows for high concentrated thermal power plants," in *Proceedings of SolarPACES 2009* (Berlin, Germany, 2009).

[4] M. Lubkoll, T. W. von Backström, and D. G. Kröger, "Survey on Pressurized Air Receiver Development," in *Proceedings of SASEC 2014* (Port Elizabeth, South Africa, 2014).

[5] SOLGATE Report, "Solar hybrid gas turbine electric power system," Tech. Rep. (European Commission, Brussels, Belgium, 2005).

[6] H. Kretzschmar and P. Gauché, "Hybrid Pressurized Air Receiver for the SUNSPOT Cycle," in *Proceedings of SASEC 2012* (Stellenbosch, South Africa, 2012).

[7] L. Heller and P. Gauché, Energy Procedia **49**, 1400–1409 (2014).

[8] B. Hoffschmidt, F. M. Tellez, A. Valverde, J. Fernandez, and V. Fernandez, Journal of Solar Energy Engineering **125**, p. 87 (2003).

[9] L. Amsbeck, G. Helsch, M. Röger, and R. Uhlig, "Development of a Broadband Antireflection Coated Transparent Silica Window for a Solar-Hybrid Microturbine System," in *Proceedings of SolarPACES 2009* (Berlin, Germany, 2009), pp. 1–10.

[10] L. Heller and J. Hoffmann, Energy Procedia **69**, 1287–1295 (2015).

[11] R. Uhlig, B. Gobereit, and J. Rheinländer, Energy Procedia **69**, 563–572 (2015).

[12] SIEMENS AG, "SGT-100 Industrial Gas Turbine," Tech. Rep. (2005).

[13] DLR, "Solar-Hybrid Power and Cogeneration Plants," Tech. Rep. 019830 (Deutsches Zentrum für Luft- und Raumfahrt e.V., 2010).

[14] NREL, SolTrace Optical Modeling Software V. 2012.7.9, 2012.

[15] S. Schell, Solar Energy **85**, 614–619 (2011).

[16] C. K. Ho, A. R. Mahoney, A. Ambrosini, M. Bencomo, A. Hall, and T. N. Lambert, Journal of Solar Energy Engineering **136**, p. 014502 (2013).

[17] M. Ebert, W. Arnold, A. Avila-Marin, T. Denk, J. Hertel, A. Jensch, W. Reinalter, A. Schlierbach, and R. Uhlig, Energy Procedia **69**, 369–378 (2015).

[18] Verein Deutscher Ingenieure, *VDI Heat Atlas*, 2nd ed. (Berlin, 2010).

[19] W. Reynolds, International Journal of Heat and Mass Transfer **6**, 445–454 (1963).

[20] D. Gärtner, K. Johannsen, and H. Ramm, International Journal of Heat and Mass Transfer **17**, 1003–1018 (1974).

[21] R. Buck, C. Barth, M. Eck, and W.-D. Steinmann, Solar Energy **80**, 1249–1254 (2006).